EAST EUROPEAN JOURNAL OF PHYSICS. 4. 220-229 (2025)
DOI:10.26565/2312-4334-2025-4-19 ISSN 2312-4334

STIMULATED RAMAN SCATTERING OF HIGH-POWER BEAM IN COLLISIONAL MAGNETOPLASMA

Keshav Walia[1]*, Taranjot Singh[1], Anuj Vijay[2], Deepak Tripathi[3]
[1]*Department of Physics, DAV University Jalandhar, India*
[2]*Department of Physics, GLA University Mathura (U.P.), India-281406*
[3]*Physics Department, USAR, Guru Gobind Singh Indraprastha University, East Delhi Campus, Delhi, India-110032*
**Corresponding Author e-mail: keshavwalia86@gmail.com*
Received August 28, 2025; revised October 5, 2025; accepted October 16, 2025

The present problem investigates Stimulated Raman Scattering of high-power beam in Collisional magnetoplasma. The laser beam has two propagation modes viz. extraordinary and ordinary modes, while its transition along the direction of static magnetic fields. The carrier redistribution affected due to modification in static magnetic field. The carrier redistribution will take place due to non-uniform heating, which results in variation in density profile in a transverse direction to axis of main beam. This density profile further causes modification in all the three waves involved in the process viz. incident beam, electron plasma wave and scattered wave. Here, 2nd order ODE for beam waists of pump beam, EPW and back-scattered wave and also expression for reflectivity will be obtained and further their numerical simulations will be carried out in order to explore impact of change in laser and plasma parameters and also externally applied magnetic field on beam waists of various waves and on SRS back-reflectivity.
Keywords: *Stimulated Raman Scattering; Static magnetic field; Non-uniform heating; Scattered Wave; Back-reflectivity*
PACS: 52.38.Hb, 52.35.Mw, 52.38.Dx

1. INTRODUCTION

New developments in laser technology resulted in generation of laser beams of small duration having peak power up to petawatt range are available [1, 2]. Researchers are interested in exploring lasers interaction with plasma medium as a result of its diverse applications such as particle acceleration, laser driven fusion and new radiation sources [3-8]. Much deeper lasers transition through plasmas is chief concern in accomplishing success in these applications. Further, laser-plasma interaction generates various instabilities such as self-focusing, scattering instabilities, harmonic generation and two plasmon decay [9-22]. The laser energy is not properly transferred to plasma medium due to these instabilities [23]. The coupling efficiency between lasers and plasma can be improved by controlling these instabilities. Self-focusing and Scattering instabilities play crucial role in laser driven fusion. In Self-focusing, laser beam transition through plasmas results in change in plasma's refractive index [24]. The density gradient created in plasmas is main cause behind self-focusing. There is rise in beam's irradiance due to self-focusing. Self-focusing causes variation in beam's angular divergence. [25]. SRS causes the breaking of main beam in to electron plasma wave (EPW) and scattered wave. SRS causes reduction in amount of laser energy transferred to plasma target. Excited EPW due to SRS has phase velocity equivalent to light's speed. It could in fact accelerate electrons that can preheat fusion fuel and reduce implosion efficiency. There is major effect of focusing of beam on SRS back-reflectivity [26]. The reduction in laser-plasma coupling efficiency is found due to both self-focusing and SRS. It is essential to have some control on these instabilities for success of inertial confinement fusion. Researchers have investigated Self-focusing and Scattering instabilities of intense laser pulses in plasmas in the past [27-34]. Barr et al. [35] investigated that SRS growth rate is greatly affected due to self-focusing. Short et al. [36] investigated effect of self-focusing on SRS instability in laser driven plasmas. In their investigation, they find that self-focusing greatly enhances SRS growth rate. The novel method has been proposed for control of SRS and electron production by Dodd and Umstadter [37]. Kalmykova and Shvets have explored SRS of laser radiation in deep plasma channels [38]. They explored that there is great reduction in growth rate of SRS on account of localization of EPW. The impact of beam irradiance and electron temperature on SRS growth rate has been explored with Kirkwood et al. [39]. The impact of filamentation of beam on SRS has been explored using non-paraxial approach by using Sharma et al. [40]. The impact of filamentation of beam on EPW and SRS back-reflectivity has been explored by Purohit et al. [41]. Singh and Walia [42] investigated effect of self-focusing on SRS and observed that focusing tendency of waves involved enhances SRS back-reflectivity. Rawat et al. [43] explored joint action of relativistic-ponderomotive forces on ring rippled beam transition in unmagnetized plasma and its effect on SRS. In their case, SRS back-reflectivity is greatly reduced at larger intensities. Sharma et al. [44] explored SRS of dark hollow Gaussian beam in unmagnetized plasma. They found that there is focusing tendency and scattered power are decreased with increment in hollow Gaussian beam's order. In fact, it has been revealed from the literature that various beam profiles have been used for exploring self-focusing and SRS [45-57]. But, impact of self-focusing on SRS has not been investigated yet in cylindrical Gaussian beams in collisional magnetized plasma. So, in present work, we are investigating for first time impact of self-focusing of Gaussian laser beams in collisional magnetized plasma.

Cite as: K. Walia, T. Singh, A. Vijay, D. Tripathi, East Eur. J. Phys. 4, 220 (2025), https://doi.org/10.26565/2312-4334-2025-4-19

EPW (ω, k) interacts with main beam (ω_0, k_0) to produce scattered wave $(\omega_0 - \omega, k_0 - k)$. The case of backscattering for $k \approx 2k_0$ is considered in present case. The carrier's redistribution take place due to non-uniform heating thereby causing self-focusing. There is modification in dispersion relation connected with EPW and hence EPW also gets self-focused under suitable boundary conditions. Irradiance associated with scattered wave is directly proportional to irradiance related with main wave and EPW. So, self-focusing results in improvement in back-scattering.

2. SOLUTION OF WAVE EQUATION FOR PUMP WAVE

The laser beam having Gaussian profile is assumed to be propagating along z-axis. The direction of static magnetic field is also along z-axis. There are basically two transition modes viz. extraordinary mode and ordinary mode. The RH circularly polarized beam is described by extra-ordinary mode while LH circularly polarized beam is described by ordinary mode.

$$A_1 = E_x + iE_y \tag{1}$$

$$A_2 = E_x - iE_y \tag{2}$$

The field vector $'E'$ of beam obeys following wave equation

$$\nabla^2 E - \nabla(\nabla \cdot E) + \frac{\omega^2}{c^2}\epsilon E = 0 \tag{3}$$

In Component form, we can express Eq. (3) as

$$\frac{\partial^2 E_x}{\partial z^2} + \frac{\partial^2 E_x}{\partial y^2} - \frac{\partial}{\partial x}\left(\frac{\partial E_y}{\partial y} + \frac{\partial E_z}{\partial z}\right) = -\frac{\omega^2}{c^2}(\epsilon E)_x \tag{4}$$

$$\frac{\partial^2 E_y}{\partial z^2} + \frac{\partial^2 E_y}{\partial x^2} - \frac{\partial}{\partial y}\left(\frac{\partial E_x}{\partial x} + \frac{\partial E_z}{\partial z}\right) = -\frac{\omega^2}{c^2}(\epsilon E)_y \tag{5}$$

$$\frac{\partial^2 E_z}{\partial z^2} + \frac{\partial^2 E_z}{\partial y^2} - \frac{\partial}{\partial z}\left(\frac{\partial E_x}{\partial x} + \frac{\partial E_y}{\partial y}\right) = -\frac{\omega^2}{c^2}(\epsilon E)_z \tag{6}$$

Here, we have considered that $(\nabla \cdot E) = 0$ and further we make use of the assumption that alteration in field along z-direction is more rapid.

$$\frac{\partial E_z}{\partial z} = -\frac{1}{\epsilon_z}\left(\epsilon_x \frac{\partial E_x}{\partial x} + \epsilon_x \frac{\partial E_y}{\partial x} + \epsilon_y \frac{\partial E_x}{\partial y} + \epsilon_y \frac{\partial E_y}{\partial y}\right) \tag{7}$$

The term $\pm i$ is multiplied with Eq. (7) and resultant is added to Eq. (4), one can easily get

$$\frac{\partial^2 A_1}{\partial z^2} + \frac{1}{2}\left(1 + \frac{\epsilon_{0+}}{\epsilon_{0z}}\right)\left(\frac{\partial^2}{\partial x^2} + \frac{\partial^2}{\partial y^2}\right)A_1 + \frac{1}{2}\left(-1 + \frac{\epsilon_{0+}}{\epsilon_{0z}}\right)\left(\frac{\partial}{\partial x} + i\frac{\partial}{\partial y}\right)^2 A_2 + \frac{\omega^2}{c^2} \times [\epsilon_{0+} + \phi_+(A_1A_1^*, A_2A_2^*)]A_1 = 0 \tag{8}$$

$$\frac{\partial^2 A_2}{\partial z^2} + \frac{1}{2}\left(1 + \frac{\epsilon_{0-}}{\epsilon_{0z}}\right)\left(\frac{\partial^2}{\partial x^2} + \frac{\partial^2}{\partial y^2}\right)A_2 + \frac{1}{2}\left(-1 + \frac{\epsilon_{0-}}{\epsilon_{0z}}\right)\left(\frac{\partial}{\partial x} - i\frac{\partial}{\partial y}\right)^2 A_1 + \frac{\omega^2}{c^2} \times [\epsilon_{0-} + \phi_-(A_1A_1^*, A_2A_2^*)]A_2 = 0 \tag{9}$$

Eqs. (8) and (9) are coupled with each other, but there exists a very weak coupling between them. So, one of the term can be set equal to zero. Assuming $A_2 \approx 0$. We can write for Eq. (8) as

$$\frac{\partial^2 A_1}{\partial z^2} + \frac{1}{2}\left(1 + \frac{\epsilon_{0+}}{\epsilon_{0z}}\right)\left(\frac{\partial^2}{\partial x^2} + \frac{\partial^2}{\partial y^2}\right)A_1 + \frac{\omega^2}{c^2} \times [\epsilon_{0+} + \phi_+(A_1A_1^*, A_2A_2^*)]A_1 = 0 \tag{10}$$

In Eq. (10), if we substitute $A_1 = A\,exp[i(\omega t - k_+ z)]$ and further make use of WKB approach, one can get

$$-2ik_+\frac{\partial A}{\partial z} + \frac{1}{2}\left(1 + \frac{\varepsilon_{0+}}{\varepsilon_{0zz}}\right)\left(\frac{\partial^2 A}{\partial x^2} + \frac{\partial^2 A}{\partial y^2}\right) + \frac{\omega^2}{c^2}\phi_+(AA^*)A = 0 \tag{11}$$

In Eq. (11), $\varepsilon_{0+} = 1 - \frac{\omega_p^2}{\omega_0(\omega_0 - \omega_c)}$, $\varepsilon_{0zz} = 1 - \frac{\omega_p^2}{\omega_0^2}$. $\omega_p = \sqrt{\frac{4\pi n_o e^2}{m}}$ is known as plasma frequency. The nonlinear part of the dielectric function for collisional magnetized plasma may be expressed as [58]

$$\varphi_+(|A.A^*|) = \frac{\omega_p^2}{\omega_0\,(\omega_0 - \omega_c)}\left(1 - \frac{2}{2 + \frac{\alpha A.A^*}{\left(1 - \frac{\omega_c}{\omega_0}\right)^2}}\right) \tag{12}$$

In Eq. (12), the nonlinear coefficient $'\alpha'$ is expressed as $\alpha = \frac{8}{3}\left(\frac{M}{m}\right)\alpha_0$ with $\alpha_0 = \frac{e^2}{8m\omega_0^2 K_B T_0}$. Here, electronic mass, ionic mass, Boltzmann constant and plasma equilibrium temperature are expressed as m, M, K_B and T_0 respectively. Now, following [58-59], Eq. (11) has solution given by

$$A = A_0(r,z)e^{-ik_0 S(r,z)} \tag{13}$$

$$A_0^2 = \frac{E_{00}^2}{f_0^2} exp\left[-\frac{r^2}{r_0^2 f_0^2}\right] \tag{14}$$

$$S = \frac{1}{2} r^2 \frac{1}{\left(1+\frac{\varepsilon_O}{\varepsilon_{Ozz}}\right)} \frac{1}{f_0} \frac{df_0}{dz} + \Phi_0(z) \tag{15}$$

$$k_0 = \frac{\omega_0}{c}\sqrt{\varepsilon_0} \tag{16}$$

In Eq. (15), the symbols ' S ' and $\Phi_0(z)$ denote Eikonal of beam and phase shift respectively. The phase shift analysis is not required in current problem. The beam width f_0 satisfied the following 2nd order differential equation,

$$\frac{d^2 f}{dz^2} = \left(1+\frac{\varepsilon_o}{\varepsilon_{Ozz}}\right)^2 \frac{1}{r_0^4 f_0^3 k_0^2} - \left(1+\frac{\varepsilon_o}{\varepsilon_{Ozz}}\right) \frac{\omega_p^2}{\varepsilon_O \omega_0^2} \frac{\alpha E_{00}^2}{r_0^2 f^3} \left(\frac{\left(1-\frac{\omega_c}{\omega_0}\right)}{\left(2\left(1-\frac{\omega_c}{\omega_0}\right)^2 + \frac{\alpha E_{00}^2}{f^2}\right)^2} \right) \tag{17}$$

In Eq. (17), ‘z’ denotes propagation axis. The boundary condition used in this case is $f = 1$ and $\frac{df}{dz} = 0$ at z=0.

3. Electron Plasma Wave Excitation

Nonlinear interaction of EPW and pump wave leads to its excitation. The excitation process of EPW in collisional magnetized plasma can be studied through following standard equations;

(a) Continuity Equation

$$\frac{\partial N}{\partial t} + \nabla \cdot (NV) = 0 \tag{18}$$

(b) Equation of motion

$$m\left[\frac{\partial V}{\partial t} + (V\cdot\nabla)V\right] = -e\left[E + \frac{1}{c}(V\times B)\right] - 2\Gamma m V - \frac{\gamma_e}{N}\nabla P \tag{19}$$

(c) Poisson’s equation

$$\nabla \cdot E = -4\pi e N \tag{20}$$

In above Eqs., instantaneous electron density, fluid velocity, Landau damping parameter and pressure term are expressed by N, V, Γ, and P respectively. For electron gas $\gamma_e = 3$. Further, by using perturbation analysis and standard approach, one can obtain the following equation denoting the change in electron density as

$$\frac{\partial^2 n}{\partial t^2} + 2\Gamma\frac{\partial n}{\partial t} - 3v_{th}^2 \nabla^2 n + \omega_p^2 \frac{N_{0e}}{N_0} n = 0 \tag{21}$$

Following [58-59], Solution of Eq. (21) is shown as

$$n = n_0(r,z) exp[i(\omega t - k(z + S(r,z)))] \tag{22}$$

$$n_0^2 = \frac{n_{00}^2}{f^2} \exp\left(-\frac{r^2}{a^2 f^2} - 2k_i z\right) \tag{23}$$

$$S = \frac{1}{2} r^2 \frac{1}{f}\frac{df}{dz} + \Phi(z) \tag{24}$$

$$\omega^2 = \omega_p^2 \frac{N_{0e}}{N_0} + 3k^2 v_{th}^2 \tag{25}$$

In above Eqs., k, ω and S are for wave vector, angular frequency and Eikonal for the EPW. Here, k_i is damping factor and $'f'$ denotes beam width of EPW and 2nd order ODE satisfied by it is expressed as

$$\frac{d^2 f}{dz^2} = \frac{1}{k^2 a^4 f^3} - \frac{\omega_p^2 f}{3k^2 v_{th}^2} \frac{\alpha E_{00}^2}{2 r_0^2 f_0^4} \left(\frac{\left(1-\frac{\omega_c}{\omega_0}\right)}{\left(2\left(1-\frac{\omega_c}{\omega_0}\right)^2 + \frac{\alpha E_{00}^2}{f^2}\right)^2} \right) \tag{26}$$

Here, the boundary condition used is $f = 0$ and $\frac{df}{dz} = 0$ at $z = 0$

4. Stimulated Raman Scattering

The total field vector E_T is expressed as sum of fields of main wave E and scattered wave E_s. i.e.

$$E_T = E\exp(i\omega_0 t) + E_s\exp(i\omega_s t) \tag{27}$$

Now, field vector E_T satisfies following wave equation

$$\nabla^2 E_T - \nabla(\nabla\cdot E_T) = \frac{1}{c^2}\frac{\partial^2 E_T}{\partial t^2} + \frac{4\pi}{c^2}\frac{\partial J_T}{\partial t} \tag{28}$$

Here, J_T is known as total current density. One can equate the scattered frequency terms to obtain following differential equation

$$\nabla^2 E_s + \frac{\omega_S^2}{c^2}\left[1 - \frac{\omega_p^2}{\omega_S^2}\frac{N_{0e}}{\gamma N_0}\right]E_s = \left[\frac{\omega_p^2\omega_s n^*}{2c^2\omega_0 N_0}\right]E_i - \nabla(\nabla\cdot E_i) \tag{29}$$

Eq. (29) has solution given by

$$E_s = E_{s0}(r,z)e^{+ik_{s0}z} + E_{s1}(r,z)e^{-ik_{s1}z} \tag{30}$$

Where $k_{S0}^2 = \frac{\omega_S^2}{c^2}\left[1 - \frac{\omega_p^2}{\omega_S^2}\right] = \frac{\omega_S^2}{c^2}\epsilon_{S0}$, with $\omega_S = \omega_0 - \omega$ and $k_{S1} = k_0 - k$.
Now, substituting Eq. (30) in Eq. (29), one can obtain

$$-k_{S0}^2 E_{S0}^2 + 2ik_{S0}\frac{\partial E_{S0}}{\partial z} + \left(\frac{\partial^2 E_{S0}}{\partial r^2} + \frac{1}{r}\frac{\partial E_{S0}}{\partial r}\right) + \frac{\omega_S^2}{c^2}\left[\epsilon_{S0} + \frac{\omega_p^2}{\omega_S^2}\left(1 - \frac{N_{0e}}{N_0}\right)\right]E_{S0} = 0 \tag{31}$$

$$-k_{S1}^2 E_{S1}^2 + 2ik_{S1}\frac{\partial E_{S1}}{\partial z} + \left(\frac{\partial^2 E_{S1}}{\partial r^2} + \frac{1}{r}\frac{\partial E_{S1}}{\partial r}\right) + \frac{\omega_S^2}{c^2}\left[\epsilon_{S0} + \frac{\omega_p^2}{\omega_S^2}\left(1 - \frac{N_{0e}}{N_0}\right)\right]E_{S1} = \frac{1}{2}\frac{\omega_p^2}{c^2}\frac{n^*}{N_0}\frac{\omega_S}{\omega_0}E_0 exp(-ik_0 S_0) \tag{32}$$

Now, solution of Eq. (32) is written as

$$E_{S1} = E'_{S1}(r,z)e^{-ik_0 S_0} \tag{33}$$

Now, put Eq. (33) in Eq. (32) and ignoring space derivatives

$$E'_{S1} = -\frac{1}{2}\frac{\omega_p^2}{c^2}\frac{n^*}{N_0}\frac{\omega_S}{\omega_0}\frac{\hat{E}E_0}{\left[k_{S1}^2 - k_{S0}^2 - \frac{\omega_p^2}{c^2}\left(1 - \frac{N_{0e}}{N_0}\right)\right]} \tag{34}$$

Following [58-59], Eq. (31) has solution denoted as

$$E_{S0} = E_{S00}e^{ik_{S0}S_c} \tag{35}$$

$$E_{S00}^2 = \frac{B_1^2}{f_S^2} exp\left[-\frac{r^2}{b^2 f_S^2}\right] \tag{36}$$

$$S_c = \frac{1}{2}r^2\frac{1}{f_S}\frac{df_S}{dz} + \Phi_S(z) \tag{37}$$

In Eq. (36), initial beam radius for scattered wave is denoted by b and beam width of scattered wave is represented by f_s and 2nd order ODE satisfies by it is represented as

$$\frac{d^2 f_s}{dz^2} = \frac{1}{k_{S0}^2 b^4 f_S^3} - \frac{\omega_p^2}{\omega_S^2\varepsilon_{S0}}\frac{\alpha E_{00}^2 f_S}{2r_0^2 f_0^4}\left(\frac{\left(1 - \frac{\omega_c}{\omega_0}\right)}{\left(2\left(1 - \frac{\omega_c}{\omega_0}\right)^2 + \frac{\alpha E_{00}^2}{f^2}\right)^2}\right) \tag{38}$$

The boundary condition used in present case is $f_s = 0$ and $\frac{df_s}{dz} = 0$ at $z = 0$.

5. Back-reflectivity

From Eq. (23), we find that EPW is damped as it transits through z-axis. So, scattered wave amplitude is decreased with increase in z. The boundary condition used is

$$E_s = E_{s0}(r,z)e^{+ik_{s0}z} + E_{s1}(r,z)e^{-ik_{s1}z} = 0 \tag{39}$$

at $z = z_c$. At $z = z_c$, scattered wave amplitude becomes zero.

$$B_1 = \frac{\omega_p^2 \omega_s N_{00}}{2c^2 \omega_0 N_0} \frac{E_{00} e^{-ik_i z_c}}{\left[k_{s1}^2 - k_{s0}^2 - \frac{\omega_p^2}{c^2}\left(1 - \frac{N_{0e}}{N_0}\right)\right]} \frac{f_s(z_c)}{f_s(z_c) f(z_c)} \frac{\exp\left(-i(k_0 S_0 + k_{s1} z_c)\right)}{\exp\left(+i(k_{s0} S_c + k_{s0} z_c)\right)} \tag{40}$$

With the condition that $\frac{1}{b^2 f_s^2} = \frac{1}{a^2 f^2} + \frac{1}{r_0^2 f_0^2}$. Now, SRS back-reflectivity is expressed as,

$$R = \frac{1}{4}\left(\frac{\omega_p^2}{c^2}\right)^2 \left(\frac{\omega_s}{\omega_0}\right)^2 \left(\frac{N_{00}}{N_0}\right)^2 \frac{(L_1 - L_2 - L_3)}{\left[k_{s1}^2 - k_{s2}^2 - \frac{\omega_p^2}{c^2}\left(1 - \frac{\left(1 - \frac{\omega_c}{\omega_0}\right)}{\left(2\left(1 - \frac{\omega_c}{\omega_0}\right)^2 + \frac{\alpha E_{00}^2}{f^2}\right)^2}\right)\right]^2} \tag{41}$$

Where

$$L_1 = \left(\frac{f_s}{f_0 f}\right)^2_{z=z_c} \frac{1}{f_s^2} exp\left(-2k_i z_c - \frac{r^2}{b^2 f_s^2}\right),$$

$$L_2 = -2\left(\frac{f_s}{f_0 f}\right)_{z_c} \frac{1}{f f_0 f_s} exp\left(-\frac{r^2}{2b^2 f_s^2} - \frac{r^2}{2a^2 f^2} - \frac{r^2}{2r_0^2 f_s^2}\right) exp(-k_i(z + z_c)) Cos(k_{s0} + k_{s1})[z - z_c],$$

$$L_3 = \frac{1}{f^2 f_0^2} exp\left(-\frac{r^2}{a^2 f^2} - \frac{r^2}{r_0^2 f_s^2} - 2k_i z_c\right).$$

6. DISCUSSION

Eqs. (17), (26), (38) and (41) can't be solved analytically. So, RK4 method is used for doing their numerical calculations for the following well-established parameters;

$$\alpha E_{00}^2 = 3.0, 4.0, 5.0\ ; \frac{\omega_p^2}{\omega_0^2} = 0.10, 0.15, 0.20\ ; \frac{\omega_c}{\omega_0} = 0.04, 0.08 \text{ and } 0.12$$

Eqs. (17), (26) and (38) are the 2nd order ODE representing the focusing/defocusing behavior of main beam, EPW and scattered wave as they transit inside plasma. In each equation, two terms are present on RHS of each equation. 1st term being diffractive term, while 2nd term being nonlinear refractive term. When 1st term is dominating, then defocusing of beams take place. When 2nd term is dominating, then focusing of beam takes place. It must also be noted that there is always change in relative magnitudes of these terms with propagation distance. All the equations have been numerically solved using RK4 method.

Figures 1, 2 and 3 denote variation of beam widths f_0 , f and f_s with dimensionless propagation distance $\eta(= z/k_0 r_0^2)$. Here, only change in beam intensity parameter αE_{00}^2 is considered whereas other parameters are kept fixed. Here, $\alpha E_{00}^2 = 3.0, 4.0$ and 5.0 are denoted by Black, Green and Red curves. The focusing tendency of various beams involved is decreased with increase in beam intensity αE_{00}^2 as a result of supremacy of divergence term over converging term with rise in αE_{00}^2 parameter. The refractive index gets reduced with rise in αE_{00}^2 parameter thereby weakening beam focusing.

Figures 4, 5 and 6 denote variation of beam widths f_0 , f and f_s with dimensionless propagation distance $\eta(= z/k_0 r_0^2)$. Here, only change in plasma density parameter $\frac{\omega_p^2}{\omega_0^2}$ is considered whereas other parameters are kept fixed. Here, $\frac{\omega_p^2}{\omega_0^2} = 0.10, 0.15, 0.20$ are denoted by Black, Green and Red curves. The focusing tendency of various beams is increased with increase in plasma density $\frac{\omega_p^2}{\omega_0^2}$ as a result of supremacy of converging term over diffraction term with rise in $\frac{\omega_p^2}{\omega_0^2}$ parameter. The refractive index gets enhanced with rise in $\frac{\omega_p^2}{\omega_0^2}$ parameter thereby strengthening beam focusing.

Figures 7, 8 and 9 denote variation of beam widths f_0 , f and f_s with dimensionless propagation distance $\eta(= z/k_0 r_0^2)$. Here, only change in cyclotron frequency parameter $\frac{\omega_c}{\omega_0}$ is considered whereas other parameters are kept fixed. Here, $\frac{\omega_c}{\omega_0} = 0.04, 0.08$ and 0.12 are denoted by Black, Green and Red curves. The focusing tendency of various beams involved is increased with increase in cyclotron frequency $\frac{\omega_c}{\omega_0}$ as a result of supremacy of converging term over diffraction term with rise in $\frac{\omega_c}{\omega_0}$ parameter. The refractive index gets enhanced with rise in $\frac{\omega_c}{\omega_0}$ parameter thereby strengthening beam focusing.

Figure 10 denotes variation of SRS back-reflectivity with dimensionless propagation distance $\eta(= z/k_0 r_0^2)$. Here, only change in beam intensity parameter αE_{00}^2 is considered whereas other parameters are kept fixed. Here, $\alpha E_{00}^2 =$

3.0 and 5.0 are denoted by Blue and Red curves. SRS back-reflectivity is found to decrease with increase in laser intensity αE_{00}^2. The reason behind it is that SRS back-reflectivity is directly linked with focusing tendency of waves involved. Since, focusing tendency of waves is decreased with rise in laser intensity αE_{00}^2. So, SRS back-reflectivity is decreased accordingly.

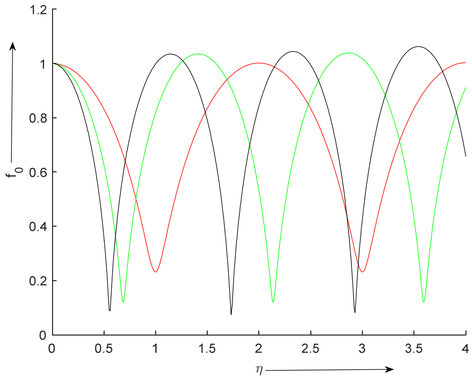

Figure 1. Variation of beam width f_0 with dimensionless propagation distance $\eta(= z/k_0 r_0^2)$. Here, $\alpha E_{00}^2 = 3.0, 4.0$ and 5.0 are denoted by Black, Green and Red curves

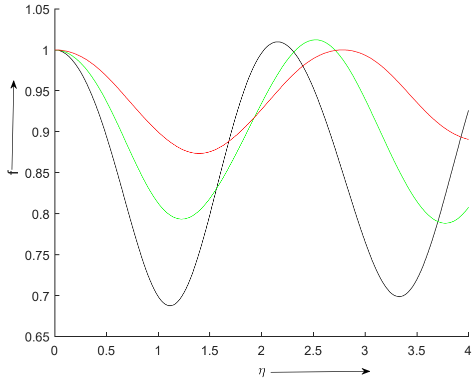

Figure 2. Variation of beam width f with dimensionless propagation distance $\eta(= z/k_0 r_0^2)$. Here, $\alpha E_{00}^2 = 3.0, 4.0$ and 5.0 are denoted by Black, Green and Red curves

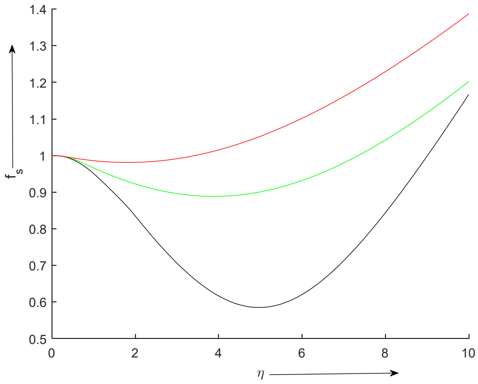

Figure 3. Variation of beam width f_s with dimensionless propagation distance $\eta(= z/k_0 r_0^2)$. Here, $\alpha E_{00}^2 = 3.0, 4.0$ and 5.0 are denoted by Black, Green and Red curves

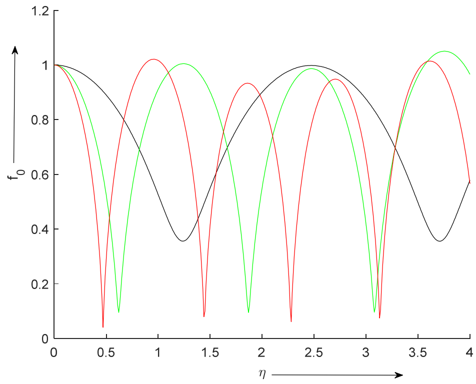

Figure 4. Variation of beam width f_0 with dimensionless propagation distance $\eta(= z/k_0 r_0^2)$. Here, $\frac{\omega_p^2}{\omega_0^2} = 0.10, 0.15, 0.20$ are denoted by Black, Green and Red curves

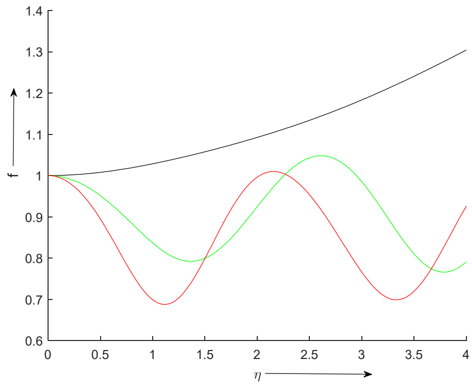

Figure 5. Variation of beam width f with dimensionless propagation distance $\eta(= z/k_0 r_0^2)$. Here, $\frac{\omega_p^2}{\omega_0^2} = 0.10, 0.15, 0.20$ are denoted by Black, Green and Red curves

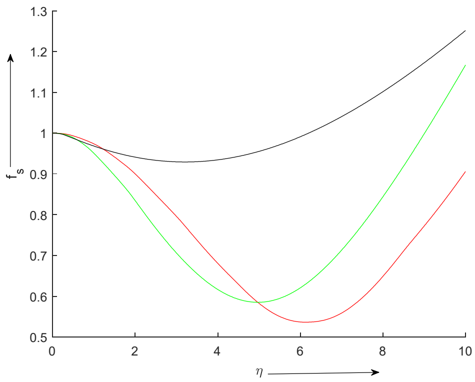

Figure 6. Variation of beam width f_s with dimensionless propagation distance $\eta(= z/k_0 r_0^2)$. Here, $\frac{\omega_p^2}{\omega_0^2} = 0.10, 0.15, 0.20$ are denoted by Black, Green and Red curves

Figure 11 denotes variation of SRS back-reflectivity with dimensionless propagation distance $\eta(= z/k_0 r_0^2)$. Here, only change in plasma density $\frac{\omega_p^2}{\omega_0^2}$ is considered whereas other parameters are kept fixed. Here, $\frac{\omega_p^2}{\omega_0^2} = 0.10$ and 0.20 are denoted by Blue and Red curves respectively. SRS back-reflectivity is increased with rise in plasma density $\frac{\omega_p^2}{\omega_0^2}$. The reason behind it is that SRS back-reflectivity is directly linked with focusing tendency of waves involved. Since, focusing tendency of waves is increased with rise in plasma density $\frac{\omega_p^2}{\omega_0^2}$. So, SRS back-reflectivity is increased accordingly.

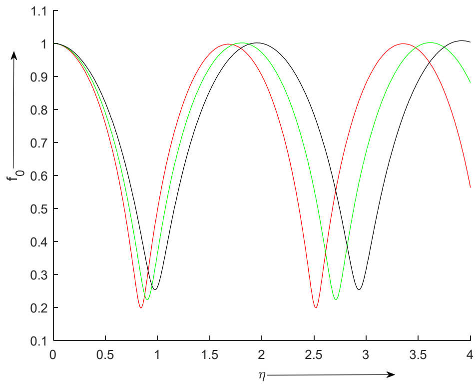

Figure 7. Variation of beam width f_0 with dimensionless propagation distance $\eta(= z/k_0r_0^2)$. Here, $\frac{\omega_c}{\omega_0} = 0.04, 0.08$ and 0.12 are denoted by Black, Green and Red curves

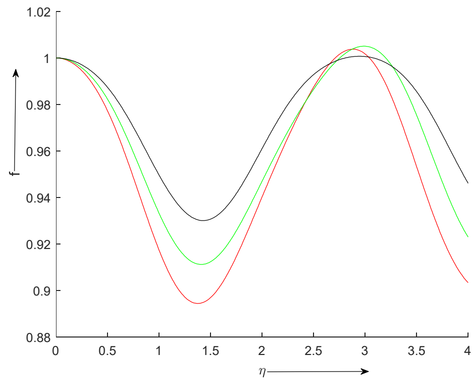

Figure 8. Variation of beam width f with dimensionless propagation distance $\eta(= z/k_0r_0^2)$. Here, $\frac{\omega_c}{\omega_0} = 0.04, 0.08$ and 0.12 are denoted by Black, Green and Red curves

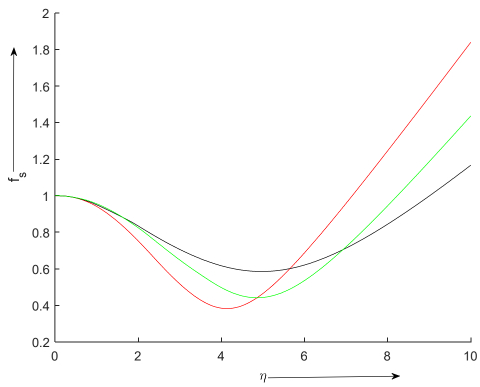

Figure 9. Variation of beam width f_s with dimensionless propagation distance $\eta(= z/k_0r_0^2)$. Here, $\frac{\omega_c}{\omega_0} = 0.04$, 0.08 and 0.12 are denoted by Black, Green and Red curves

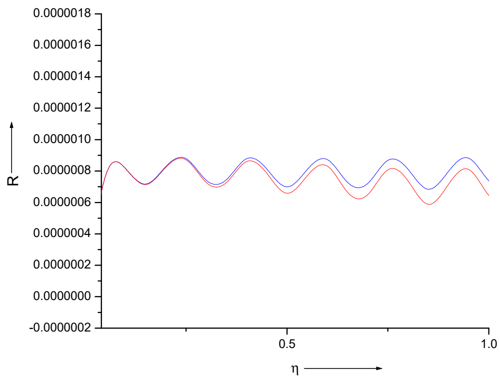

Figure 10. Variation of SRS back-reflectivity with dimensionless propagation distance $\eta(= z/k_0r_0^2)$. Here, $\alpha E_{00}^2 = 3.0$ and 5.0 are denoted by Blue and Red curves

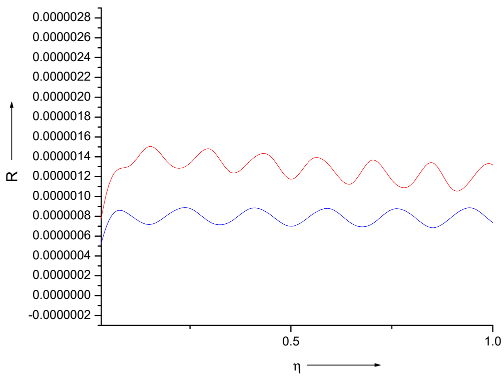

Figure 11. Variation of SRS back-reflectivity with dimensionless propagation distance $\eta(= z/k_0r_0^2)$. Here, $\frac{\omega_p^2}{\omega_0^2} = 0.10$ and 0.20 are denoted by Blue and Red curves respectively

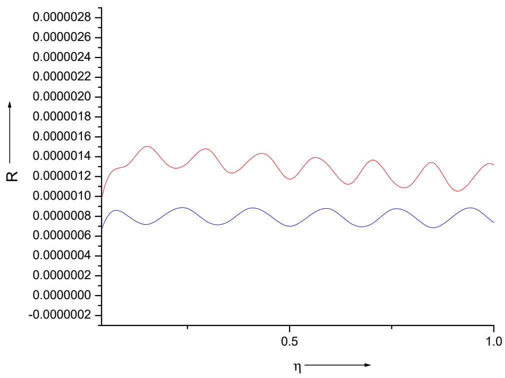

Figure 12. Variation of SRS back-reflectivity with dimensionless propagation distance $\eta(= z/k_0r_0^2)$. Here, $\frac{\omega_c}{\omega_0} = 0.04$ and 0.12 are denoted by Blue and Red curves respectively

Figure 12 denotes variation of SRS back-reflectivity with dimensionless propagation distance $\eta(= z/k_0r_0^2)$. Here, only change in cyclotron frequency $\frac{\omega_c}{\omega_0}$ is considered whereas other parameters are kept fixed. Here, $\frac{\omega_c}{\omega_0} = 0.04$ and 0.12 are denoted by blue and red curves respectively. SRS back-reflectivity is increased with rise in cyclotron frequency $\frac{\omega_c}{\omega_0}$. The reason behind it is that SRS back-reflectivity is directly linked with focusing tendency of waves involved. Since, focusing tendency of waves is increased with rise in cyclotron frequency $\frac{\omega_c}{\omega_0}$. So, SRS back-reflectivity is increased accordingly.

7. CONCLUSIONS

The present research deals with SRS of high-power beam in Collisional magnetoplasma. The results obtained from present problem are as follows:

(1) Focusing ability of various waves involved is increased with increase in plasma density, cyclotron frequency and with decrease in laser intensity. This is due to enhancement in net refractive index gradient, which strengthens beam focusing.

(2) SRS back-reflectivity is increased with rise in plasma density, cyclotron frequency and with decrease in beam intensity. This is due to enhancement in net refractive index gradient, which strengthens beam focusing and consequently amplifies SRS back-reflectivity.

Present results are really helpful in knowing physics of laser driven fusion.

ORCID

Keshav Walia, https://orcid.org/0000-0001-9547-3027; **Taranjot Singh,** https://orcid.org/0009-0009-8172-4097
Anuj Vijay, https://orcid.org/0000-0001-6610-3844; **Deepak Tripathi,** https://orcid.org/0000-0001-9945-4069

REFERENCES

[1] M.D. Perry, and G. Mourou, "Terawatt to petawatt subpicosecond lasers," Science, **264**, 917-924 (1994). https://doi.org/10.1126/science.264.5161.917
[2] T. Feder, "Petawatt laser probes nature at Texas University," Phys. Today, **61**, 27 (2008). https://doi.org/10.1063/1.3001859
[3] M. Tabak, J. Hammer, M.E. Glinsky, W.L. Kruer, S.C. Wilks, J. Woodworth, E.M. Campbell, and M.D. Perry, "Ignition and high gain with ultrapowerful lasers", Phys. Plasmas, **1**, 1626–1634 (1994). https://doi.org/10.1063/1.870664
[4] C. Deutsch, H. Furukawa, K. Mima, M. Murakami, and K. Nishihara, "Interaction physics of the fast ignitor concept," Phys. Rev. Lett. **77**, 2483-2486 (1996). https://doi.org/10.1103/PhysRevLett.77.2483
[5] E. Esarey, C.B. Schroeder, and W.P. Leemans, "Physics of laser-driven plasma-based electron accelerators," Rev. Mod. Phys. **81**, 1229-1285 (2009). https://doi.org/10.1103/revmodphys.81.1229
[6] R. Bingham, J.T. Mendonca, and P.K. Shukla, "Topical review: plasma based charged-particle accelerators," Plasma Phys. Controlled Fusion, **46**, R1 (2004). https://doi.org/10.1088/0741-3335/46/1/r01
[7] A. Rousse, "Production of a keV X-Ray Beam from synchrotron radiation in relativistic laser-plasma interaction," Phys. Rev. Lett. **93**, 135005 (2004). https://doi.org/10.1103/physrevlett.93.135005
[8] Z. Zeng, Y. Cheng, X. Song, R. Li, and Z. Xu, "Generation of an extreme ultraviolet supercontinnum in a two-color laser field," Phys. Rev. Lett. **98**, 203901 (2007). https://doi.org/10.1103/physrevlett.98.203901
[9] K. Walia, "Propagation characteristics of a high-power beam in weakly relativistic-ponderomotive thermal quantum plasma," Commun. Theor. Phys. **75**, 095501 (2023). https://doi.org/10.1088/1572-9494/accf82
[10] K. Walia, "Nonlinear interaction of high power beam in weakly relativistic and ponderomotive cold quantum plasma," Optik, **219**, 165040 (2020). https://doi.org/10.1016/j.ijleo.2020.165040
[11] K. Walia, and S. Kaur, "Nonlinear Interaction of Elliptical Laser Beam with Collisional Plasma: Effect of Linear Absorption," Commun. Theor. Phys. **65**, 78 (2016). https://doi.org/10.1088/0253-6102/65/1/78
[12] K. Walia, "Nonlinear Interaction of High Power Elliptical Laser Beam with Cold Collisionless Plasma," J. Fusion Energ. **35**, 446 (2016). https://doi.org/10.1088/0253-6102/65/1/78
[13] K. Walia, "Enhanced Brillouin scattering of Gaussian laser beam in collisional plasma: Moment theory approach," J. Nonlinear Opt. Phys. Mater. **23**, 1450011 (2014). https://doi.org/10.1142/s0218863514500118
[14] T. Singh, and K. Walia, "Second Harmonic Generation of High Power Cosh-Gaussian Beam in Thermal Quantum Plasma: Effect of Relativistic and Ponderomotive Nonlinearity," J. Contemp. Phys. **59**, 244-253 (2024). https://doi.org/10.1134/s1068337224700488
[15] K. Walia, "Self-focusing of high power beam in unmagnetized plasma and its effect on Stimulated Raman scattering process," Optik, **225**, 165592 (2021). https://doi.org/10.1016/j.ijleo.2020.165592
[16] K. Walia, "Stimulated Brillouin Scattering of high-power beam in unmagnetized plasma: Effect of relativistic and ponderomotive nonlinearities," Optik, **221**, 165365 (2020). https://doi.org/10.1016/j.ijleo.2020.165365
[17] K. Singh, and K. Walia, "Influence of Self-Focused Elliptical Laser Beam on Second Harmonic Generation in Cold Quantum Plasma," J. Contemp. Phys. **59**, 154-164 (2024). https://doi.org/10.1134/s1068337224700300
[18] K. Walia, V. Kakkar, and D. Tripathi, "Second harmonic generation of high-power laser beam in cold quantum plasma," Optik, **204**, 164150 (2020). https://doi.org/10.1016/j.ijleo.2019.164150
[19] K. Walia, N. Mehra, and S. Pandit, "Propagation Characteristics of q-Gaussian Laser Beam in Cold Collisionless Plasma," J. Contemp. Phys. **59**, 378-385 (2024). https://doi.org/10.1134/S1068337225700203
[20] V. Nanda, and N. Kant, "Enhanced relativistic self-focusing of Hermite-cosh-Gaussian laser beam in plasma under density transition," Phys. Plasmas **21**, 042101 (2014). https://doi.org/10.1063/1.4870080
[21] N. Kant, M.A. Wani, and A. Kumar, "Self-focusing of Hermite-Gaussian laser beams in plasma under plasma density ramp," Opt. Commun. **285**, 4483-4487 (2012). https://doi.org/10.1016/j.optcom.2012.05.065
[22] M.A. Wani, N. Kant, Investigation of relativistic self-focusing of Hermite-cosine-Gaussian laser beam in collisionless plasma, Optik 127, 4705(2016).

[23] W.L. Kruer, *The Physics of Laser Plasma Interactions*, (Addison-Wesley, Redwood City, 1998).
[24] W.B. Mori, C. Joshi, J.M. Dawson, D.W. Forslund, and J.M. Kindel, "Evolution of self-focusing of intense electromagnetic waves in plasma," Phys. Rev. Lett. **60**, 1298-1301 (1988). https://doi.org/10.1103/PhysRevLett.60.1298
[25] P.M. Lushnikov, and H.A. Rose, "How much laser power can propagate through fusion plasma?" Plasma Phys. Controll. Fusion **48**, 1501 (2006). https://doi.org/10.1088/0741-3335/48/10/004
[26] H.A. Salih, S.T. Mahmoud, R.P. Sharma, and M. Rafat, "Stimulated Raman Scattering of relativistic laser beam in plasmas," Phys. Plasmas **12**, 042302 (2005). https://doi.org/10.1063/1.1856480
[27] C.S. Liu, and V.K. Tripathi, "Consequence of filamentation on stimulated Raman scattering," Phys. Fluids, **29**, 4188-4191 (1986). https://doi.org/10.1063/1.865710
[28] T. Afsar-rad, S.E. Coe, O. Willi, and M. Desselberger, "Evidence of stimulated Raman scattering occurring in laser filaments in long-scale-length plasmas," Phys. Plasmas, **4**, 1301-1322 (1992). https://doi.org/10.1063/1.860086
[29] Y.H. Tang, H. Shen-Sheng, Z. Chang-Xue, W. Yan-Qing, C. Jing, Z. Fang-Chuan, Z. Yu-Zhe, X. Zhi-Zhan, "Stimulated Raman backscattering from an ultrashort laser interacting with underdense plasmas," Chin. Phys. **11**, 50 (2002). https://doi.org/10.1088/1009-1963/11/1/311
[30] R.K. Kirkwood, J.D. Moody, C. Niemann, E.A. Williams, A.B. Langdon, O.L. Landen, L. Divol, and L.J. Suter, "Observation of polarization dependent Raman scattering in a large scale plasma illuminated with multiple laser beams," Phys. Plasmas **13**, 082703 (2006). https://doi.org/10.1063/1.2215415
[31] L. Yin, B.J. Albright, H.A. Rose, K.J. Bowers, B. Bergen, D.S. Montgomery, J.L. Kline, and J.C. Fernandez, "Onset and saturation of backward stimulated Raman scattering of laser in trapping regime in three spatial dimensions," Phys. Plasmas, **16**, 113101 (2009). https://doi.org/10.1063/1.3250928
[32] D. Tripathi, T. Singh, A. Vijay, and K. Walia, "Second Harmonic Generation of q-Gaussian Laser Beam in Thermal Quantum Plasma," J. Contemp. Phys. **60**, 171-180 (2025). https://doi.org/10.1134/s1068337225700574
[33] D. Tripathi, S. Kaur, A. Vijay, and K. Walia, "Nonlinear Dynamics of q-Gaussian Laser Beam in Collisional Plasma: Effect of Linear Absorption," J. Contemp. Phys. **60**, 16-23 (2025). https://doi.org/10.1134/s1068337225700409
[34] K. Singh, and K. Walia, "Impact of High-Power Cosh-Gaussian Beam on Second Harmonic Generation in Collisionless Magnetoplasma," J. Contemp. Phys. **59**, 254-264 (2024). https://doi.org/10.1134/s106833722470049x
[35] H.C. Barr, T.J.M. Boyd, and G.A. Coutts, "Stimulated Raman Scattering in the presence of filamentation in underdense plasmas," Phys. Rev. Lett. **56**, 2256-2259 (1986). https://doi.org/10.1103/PhysRevLett.56.2256
[36] R.W. Short, W. Seka, and R. Bahr, "Stimulated Raman scattering in self-focused light filaments in laser-produced plasmas," Phys. Fluids **30**, 3245-3251 (1987). https://doi.org/10.1063/1.866499
[37] E.S. Dodd, and D. Umstadter, "Coherent control of stimulated Raman scattering using chirped laser pulses," Phys. Plasmas, **8**, 3531-3534 (2001). https://doi.org/10.1063/1.1382820
[38] Y.S. Kalmykov, and G. Shvets, "Stimulated Raman backscattering of laser radiation in deep plasma channels," Phys. Plasmas, **11**, 4686-4694 (2004). https://doi.org/10.1063/1.1778743
[39] R.K. Kirkwood, R.L. Berger, C.G.R. Geddes, J.D. Moody, B.J. Macgowan, S.H. Glenzer, K.G. Estabrook, *et al*., "Scaling of saturated stimulated Raman scattering with temperature and intensity in ignition scale plasmas," Phys. Plasmas, **10**, 2948-2955 (2003). https://doi.org/10.1063/1.1580814
[40] P. Sharma, and R.P. Sharma, "Suppression of stimulated Raman scattering due to localization of electron plasma wave in laser beam filaments," Phys. Plasmas, **16**, 032301 (2009). https://doi.org/10.1063/1.3077670
[41] G. Purohit, P. Sharma, and R.P. Sharma, "Filamentation of laser beam and suppression of stimulated Raman scattering due to localization of electron plasma wave," J. Plasma Phys. **78**, 55-63 (2012). https://doi.org/10.1017/S0022377811000419
[42] A. Singh, and K. Walia, "Self-focusing of Gaussian laser beam in collisionless plasma and its effect on stimulated Raman scattering process," Optik, **124**, 6074-6080 (2013). https://doi.org/10.1016/j.ijleo.2013.07.005
[43] P. Rawat, R. Gauniyal, and G. Purohit, "Growth of ring ripple in a collisionless plasma in relativistic-ponderomotive regime and its effect on stimulated Raman backscattering process," Phys. Plasmas, **21**, 062109 (2014). https://doi.org/10.1063/1.4883221
[44] P. Sharma, "Stimulated Raman scattering of ultra intense hollow Gaussian beam in relativistic plasma," Laser Part. Beams **33**, 489-498 (2015). https://doi.org/10.1017/S0263034615000488
[45] T.W. Huang, C.T. Zhou, A.P.L. Robinson, B. Qiao, H. Zhang, S.Z. Wu, H.B. Zhou, *et al*., "Mitigating the relativistic laser beam filamentation via an elliptical beam profile," Phys. Rev. E, **92**, 053106 (2015). https://doi.org/10.1103/PhysRevE.92.053106
[46] H.S. Brandi, C. Manus, and G. Mainfray, "Relativistic and ponderomotive self-focusing of a laser beam in a radially inhomogeneous plasma. I. Paraxial approximation," Phys. Fluids B, **5**, 3539-3550 (1993). https://doi.org/10.1063/1.860828
[47] H.S. Brandi, C. Manus, G. Mainfray, and T. Lehner, "Relativistic self-focusing of ultraintense laser pulses in inhomogeneous underdense plasmas," Phys. Rev. E, **47**, 3780-3783 (1993). https://doi.org/10.1103/PhysRevE.47.3780
[48] J.F. Drake, P.K. Kaw, Y.C. Lee, G. Schmid, C.S.L. Marshall, and N. Rosenbluth, "Parametric instabilities of electromagnetic waves in plasmas," Phys. Fluids, **17**, 778-785 (1974). https://doi.org/10.1063/1.1694789
[49] M.S. Sodha, G. Umesh, and R.P. Sharma, "Enhanced Raman scattering of a Gaussian laser beam from a plasma," Plasma Phys. **21**, 687 (1979). https://doi.org/10.1088/0032-1028/21/8/002
[50] R.K. Singh, and R.P. Sharma, "Stimulated Raman backscattering of filamented hollow Gaussian beams," Laser Part. Beams, **31**, 387-394 (2013). https://doi.org/10.1017/s0263034613000384
[51] N.S. Saini, and T.S. Gill, "Enhanced Raman scattering of a rippled laser beam in a magnetized collisional plasma," Laser Part. Beams, **22**, 35-40 (2004). https://doi.org/10.1017/S0263034604221073
[52] P. Jha, G. Raj, and A.K. Upadhyaya, "Relativistic and ponderomotive effects on stimulated Raman scattering of intense laser radiation in plasma," IEEE Trans. Plasma Sci. **34**, 922-926 (2006). https://doi.org/10.1109/tps.2006.878144
[53] R.P. Sharma, and M.K. Gupta, "Effect of relativistic and ponderomotive nonlinearities on stimulated Raman scattering in laser plasma interaction," Phys. Plasmas, **13**, 113109 (2006). https://doi.org/10.1063/1.2357895
[54] F. Cornolti, M. Lucchesi, and B. Zambon, "Elliptic Gaussian beam self-focusing in nonlinear media," Optics Comm. **75**, 129-1356 (1990). https://doi.org/10.1016/0030-4018(90)90241-K

[55] S. Konar, and A. Sengupta, "Propagation of an elliptic Gaussian laser beam in a medium with saturable nonlinearity," J. Opt. Soc. Am. B, **11**, 1644-1646 (1994). https://doi.org/10.1364/JOSAB.11.001644
[56] G. Fibich, and B. Ilan, "Self-focusing of elliptic beams: an example of the failure of the aberrationless approximation," J. Opt. Soc. Am. B, **17**, 1749-1758 (2000). https://doi.org/10.1364/JOSAB.17.001749
[57] T.S. Gill, N.S. Saini, S.S. Kaul, and A. Singh, "Propagation of elliptical Gaussian laser beam in a higher order non-linear medium," Optik, **115**, 493-498 (2004). https://doi.org/10.1078/0030-4026-00405
[58] S.A. Akhmanov, A.P. Sukhorokov, and R.V. Kokhlov, "Self-focusing and diffraction of light in nonlinear medium," Sov. Phys. Uspekhi, **10**, 609(1968).
[59] M.S. Sodha, A.K. Ghatak, and V.K. Tripathi, "Self focusing of laser beams in plasmas and semiconductors," Progress in Optics **13**, 169-265 (1976). https://doi.org/10.1016/S0079-6638(08)70021-0

ВИМУШЕНЕ КОМБІНАЦІЙНЕ РОЗСІЮВАННЯ ПОТУЖНОГО ПУЧКА У МАГНІТОПЛАЗМІ ІЗ ЗІТКНЕННЯМИ

Кешав Валья[1], Таранджот Сінгх[1], Анудж Віджай[2], Діпак Тріпаті[3]
[1]Кафедра фізики, Університет DAV, Джаландхар, Індія
[2]Кафедра фізики, Університет GLA, Матхура (У.П.), Індія-281406
[3]Кафедра фізики, USAR, Університет Гуру Гобінда Сінгха Індрапрастхи, кампус Східного Делі, Делі, Індія-110032

У цій задачі досліджується вимушене комбінаційне розсіювання потужного променя в зіткнювальній магнітоплазмі. Лазерний промінь має два режими поширення, а саме: незвичайний та звичайний, під час його переходу вздовж напрямку статичних магнітних полів. Перерозподіл носіїв відбувається через модифікацію статичного магнітного поля. Перерозподіл носіїв відбувається через неоднорідне нагрівання, що призводить до зміни профілю густини в поперечному напрямку до осі основного променя. Цей профіль густини додатково викликає модифікацію всіх трьох хвиль, що беруть участь у процесі, а саме: падаючого променя, електронної плазмової хвилі та розсіяної хвилі. Тут будуть отримані ЗДР 2-го порядку для перетяжок пучка накачування, електроплівкової хвилі та хвилі зворотного розсіяння, а також вираз для відбивної здатності, і далі буде проведено їх числове моделювання, щоб дослідити вплив зміни параметрів лазера та плазми, а також зовнішнього прикладеного магнітного поля на перетяжки пучка різних хвиль та на зворотну відбивну здатність ВКР.

Ключові слова: *вимушене комбінаційне розсіювання; статичне магнітне поле; неоднорідний нагрів; розсіяна хвиля; зворотна відбивна здатність*